Dynamic photoinduced anisotropy in PMMA/disperse red 13 thin films

B. ABBAS*, M. ALSHIKH KHALIL
Department of Physics, Atomic Energy Commission, P. O. Box 6091, Damascus, Syria

The photoinduced anisotropy's dynamics of PMMA/Disperse Red 13 (PMMA/DSR13) thin films were investigated by the pump-probe method. The anisotropy increased exponentially at the start of pumping, and reached a photostationary state due to the photoisomerization process. However, anisotropy decreased exponentially as soon as the irradiation was switched off. It was concluded that the Angular Hole Burning (AHB) and the Angular Redistribution (AR) effects are responsible for the observed dynamic photoinduced anisotropy (POA). Moreover, the relative POA revealed that the photoisomer's thermal isotropic relaxation was insignificant, in comparison with the anisotropic reversible photoisomerization that occurred at cutting-off the pump.

(Received March 6, 2025; accepted December 4, 2025)

Keywords: Photoinduced anisotropy, Photoisomerization, Angular hole burning (AHB), Angular redistribution (AR)

1. Introduction

Photoinduced anisotropy in dye-doped polymers has been under intensive investigation for the last two decades. POA is a key element in the research and development of light-controlled anisotropy in materials exhibiting POA, which are intended for use in numerous photonic applications [1–2], in the field of polarization holography [3-4], and optical phase conjugation [5-7]. POA is located at the centre of the photoalignment (PA) technique, which is exploited in the industrial development of liquid crystal displays for producing superior aligning substrates [8-9]. This method avoids the problems of the old mechanical surface handling and utilizes light with linear polarization to create anisotropy in a photosensitive film. Merging the superb mechanical properties of the polymer matrices, i.e. elevated degree of chain extension and ordered structure (which acts as a host for the chromophore particles), with the optoelectronic features of organic chromophores (guest particles), dichroic polarizing films may be produced [10-11]. The integration of highly dichroic polarizing thin films may be favourably used for the construction of anisotropic linear and nonlinear optical devices [12-15], molecular strain sensors for polymeric thin films, and lasers [16–19]. In particular, substantial devotion has been paid to assembling organic molecules into polymeric films because of their possible applications for miniaturized optoelectronic devices [20-21]. In azo-based polymers, the photoisomerization encourages conformational variations in the polymer chains, which, in turn, induce macroscopic changes in the physical and chemical properties of the structure. The photoisomerization permits polymeric structures with azo molecules to be used as optical switches that may control swiftly and reversibly the material characteristics [22–23]. Photochemical *trans* ↔ *cis* isomerization, which induced by light, is one of the most significant properties of organic dyes [23]. In PMMA/DSR13 amorphous thin films, the excitation of DSR13 chromophores by polarized light leads to rapid *trans* ↔ *cis* photoisomerization to appear. This process induces, more or less, a permanent anisotropy. This phenomenon could be employed in photonic applications [24].

Extensive work has been published on the POA in several polymer/dye blends as detailed above. For example, Wu and his colleagues [25] investigated the POA dynamics of PMMA thin films doped with DSR13 chromophores at 515 nm and 375 nm pumping wavelengths, where the temporal changes in the isotropic and anisotropic absorption coefficients were measured. Their results showed that pumping with linearly polarized light at 515 nm or 375 nm, led the transmitted perpendicular component of the probe beam to decrease in the early time, and then increase towards a photostationary state. similarly, the transmitted parallel component of the probe beam increased in the early time, and then decreased to a photostationary state. The authors attributed this abnormal behaviour to the *trans* and *cis* isomer's different absorption at the pumping wavelengths, where photoisomerization has a dominant role in the beginning, but after some time, the angular redistribution effect takes the lead so that all isomers are being rotated perpendicularly to the polarization of the irradiation beam. Petris *et al.* [26] studied Disperse Red 1 (DR1) (4-[N-ethyl-N-(2-hydroxy-ethyl)]-amino-4′-nitroazobenzene) azo-dye for DNA-CTMA functionalization, which is a new deoxyribonucleic acid (DNA) based bio-material with promising applications in organic photonics and electronics, where the material's optical response at light excitation is a very important detrimental effect. They used a pump-probe interferometric method to study the spatial distribution of the optical phase change, its magnitude and its dependence on the pump intensity. They concluded that *trans-cis-trans* photoisomerization is

the dominant processes responsible for the light-induced phase modulation. These representative examples illustrate that studying POA in dye-doped polymeric thin films is fundamentally important for developing advanced photonics applications like polarization holography, optical switching, data storage, and sensors, because it allows controllable, light-induced structural changes in the material's optical properties [27]. Understanding this process allows for the accurate engineering of light-controlling elements, leading to more effective and complex optical devices, as well as offers fundamental insights into light-matter interactions and material design [28]. As per our knowledge, the POA in PMMA/DSR13 films has never been studied distinctly and deeply. In this paper, we examine the dynamic behaviour of POA of DSR13 chromophore fused into poly(methyl methacrylate) (PMMA) matrix, with specific emphasis on the DSR13 photoisomerization kinetics.

2. Experimental

Disperse Red 13 ($C_{16}H_{17}ClN_4O_3$, molecular weight: 348.787 g/mol, ~95 % dye content, Sigma-Aldrich) is an azo-derivative organic dye (Fig. 1) that was used as received. 50 ml of Dichloromethane (DCM, CH_2Cl_2, 95.5%, Sigma-Aldrich) were added to 2 gr of PMMA (PMMA, MW: 36000, Acros Organics). 0.1 gr of DSR13 was added to the mixture (PMMA-to-DSR13 ratio: 5wt%) and stirred for 4 hours, allowing the dye molecules and the polymer to fully dissolve and mix. Transparent glass substrates were used to deposit thin films by the dip-coating technique. Samples were baked in an oven at 70 ºC and kept for three hours in order to eliminate any residual solvent. Lastly, a desiccator was used to store the samples in a dark environment at 22ºC. Prism Coupling Technique was used to measure the films' thicknesses, and they were of the order of 1 μm. The absorption spectra of the samples were acquired by a UV-visible spectrophotometer (Specord S100, from Analytik Jena).

Fig. 1 illustrates that the wavelength 514 nm is quite appropriate for pump-probe irradiation for investigating PMMA/DSR13 thin films. This wavelength corresponds to the maximum absorption of DSR13. Fig. 2 shows the experimental set up for POA measurements. The samples were pumped by an Ar^+ laser beam (543-MAP-A02, Melles Griot). The probe beams' polarizations were chosen so that one of them was with a linear polarization parallel to the linear polarization of the pump, and the other beam had its linear polarization direction perpendicular to the direction of the linear polarization of the pump, and were used at the same time. The probe beams passed through the thin films, and get incident onto two photodiodes, which were connected to a PC through two low-noise preamplifiers (SR570, SR Systems), and two DSP lock-in amplifiers (SR850, SR Systems, and Signal Recovery 7280). This formation allowed concurrent measurements of the transmission variations of both probe beams at the same pump intensity. An IEEE 488.2 GPIB (from National Instruments) card was used to control and record the acquired data with a program written in C++.

POA is calculated using the following equation [24],

$$S_{2,\lambda} = \frac{1}{3}\left(OD_{//} - OD_{\perp}\right) \tag{1}$$

where $OD_{//}$ and $OD_{\perp}$ are the parallel and perpendicular optical densities to the pump linear polarization direction, respectively, which could be calculated by [29],

$$OD_{//} = -\log T_{//} \tag{2}$$

and

$$OD_{\perp} = -\log T_{\perp} \tag{3}$$

where $T_{//}$ and $T_{\perp}$ are the parallel and perpendicular transmitted intensities with respect to the linear polarization direction of the pump, respectively, which were calculated by [30],

$$T_{//} = \frac{I_{//}}{I_0} \tag{4}$$

and

$$T_{\perp} = \frac{I_{\perp}}{I_0} \tag{5}$$

where I_0 is the probe beam intensity in the presence of the substrate without coating. $I_{//}$ and $I_{\perp}$ are the probe beam intensities, which were transmitted through the thin film with its polarization direction parallel and perpendicular to the pump polarization, respectively.

3. Results and discussion

POA in PMMA/DSR13 thin film is illustrated in Fig. 3. This figure shows the dynamic growth of the anisotropy in the thin film. In the first 1000 seconds, fast growth of the anisotropy was an indication of the angular hole burning (AHB) prevalence which is due to the drift of most *trans* molecules to the *cis* state [31]. The following slow increase shows the prevalence of the angular redistribution (AR) effect, by which *trans* molecules progressively accumulate perpendicular to the electric vector direction of the pump [32]. Moreover, it removes partially the anisotropy in *cis* form, upon which the $\cos^2\theta$ absorption probability of the angular distribution in *trans*, becomes flat [24]. At the saturation stage, AHB and AR effects get into a balance state, at which the conversion *trans* ↔ *cis* remains predominant. Cutting-off the pump leads to an exponential decline in anisotropy, indicating a sudden collapse in the *cis* population in the beginning in addition to a collapse in the photoinduced polar order.

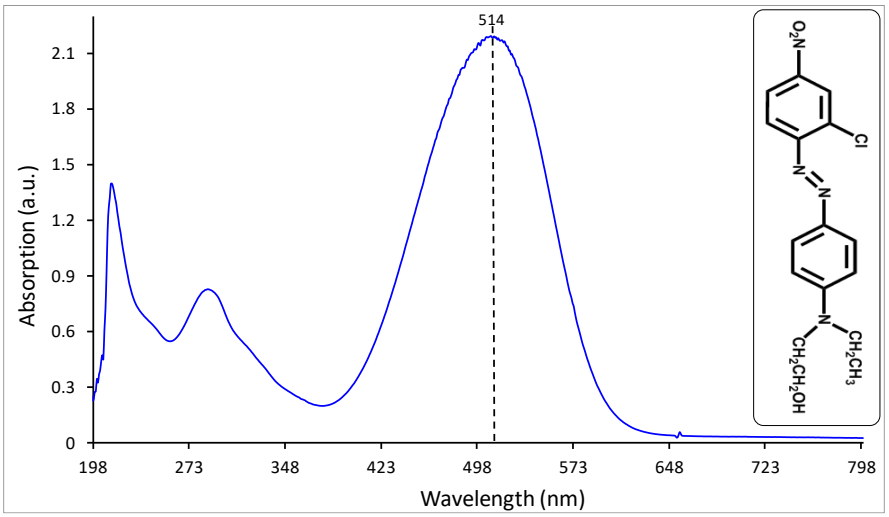

Fig. 1. UV-Visible absorption spectrum of a PMMA/DSR13 thin film. The inset displays the chemical structure of DSR13 (colour online)

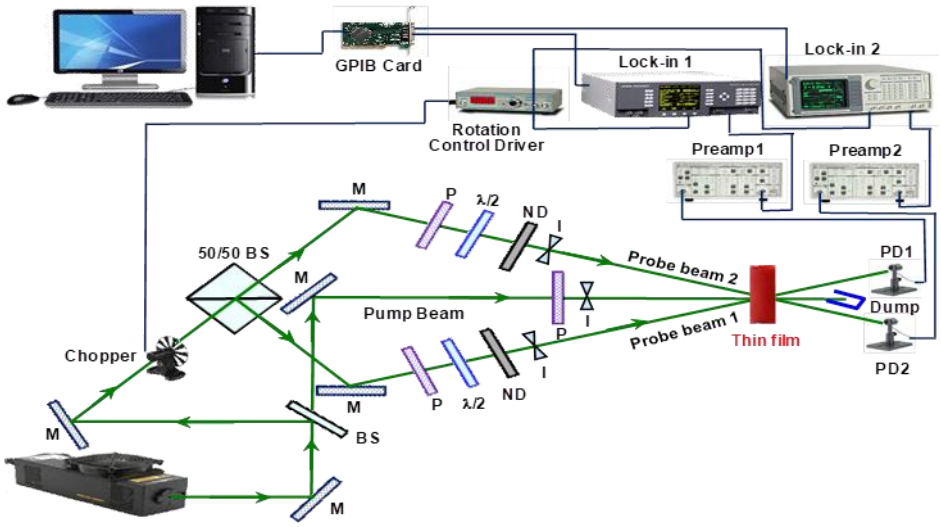

Fig. 2. The experimental setup: P: polarizer, ND: neutral density filter, B/S: beam splitter, λ/2 half-wave plate, I: iris, P: polarizer, M: mirror and PD: photodiode (colour online)

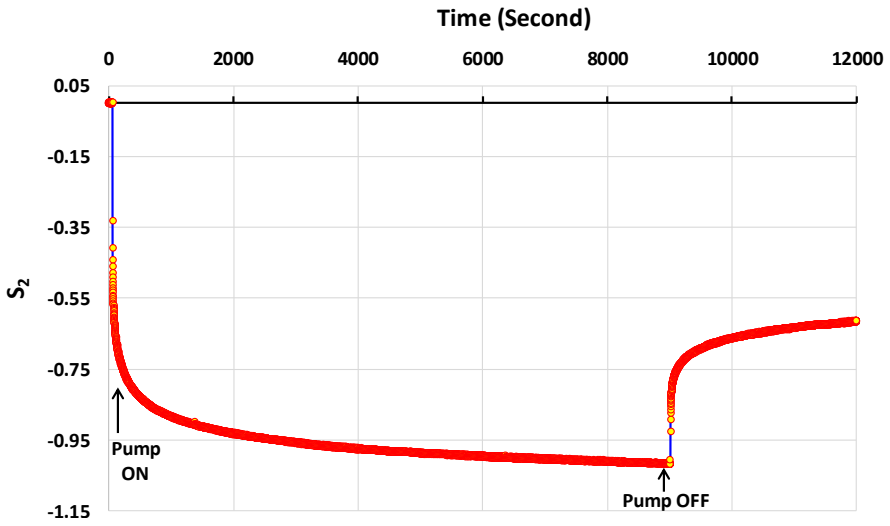

Fig. 3. The dynamic growth of POA in PMMA/DSR13 thin film at 5 mW pump intensity (colour online)

The slow decrease indicates the evanescence of the *trans* chromophores from their photoinduced polar orientation, and forms a further thermodynamically stable assembly.

Growth and relaxation of the POA (Fig. 3) shows that this anisotropy is stable, for guest-host PMMA/DSR13 samples, which reflects a strong AR and a slow *trans* angular diffusion due to the bulky size of *trans* molecules as well as the high glass transition temperature of the guest, which is $T_g = 95^{\circ}C$ [24].

The analysis of the anisotropy growth reveals two characteristic styles, namely, fast and slow modes, which can be fitted by Kohlrausch–Williams–Watts (KWW) exponential equation [33], which is given as,

$$S_2(t) = S_{2o} \exp\left[-\left(\frac{t}{\tau}\right)^{\beta}\right] \tag{6}$$

Here, t is the time at which $S_2(t)$ was measured. S_{2o} is the sample anisotropy prior to sample irradiation. τ is the characteristic rise time. β (0≤β≤1) is a distribution parameter which describes the distribution breadth of the rise time. For example, β=1 refers to a simple exponential rise, whereas smaller β refers to a broader distribution, while β=0 describes the rise of a widespread range of exponential functions with diverse rise times. The rise time constant can be deduced using equation (6) by taking its logarithm twice and plotting $\ln(t)$ versus $\ln\left[-\ln\left(\frac{S_2(t)}{S_{2o}}\right)\right]$, whereby a straight line is plotted whose gradient gives $\frac{1}{\beta}$ and the intercept yields $\ln(\tau)$ [34].

The results of this approach are shown in Fig. 4 using a 1.5μm PMMA/DSR13 thin film as a representative sample, and summarized in Table 1. Here, β is less than unity, which indicates that the motion of chromophores is very much dependent on the local surroundings of each molecule. As such, the general rise function is thought of as a sum of many exponential rises, which are expressed via the stretched equation (Eq. 6).

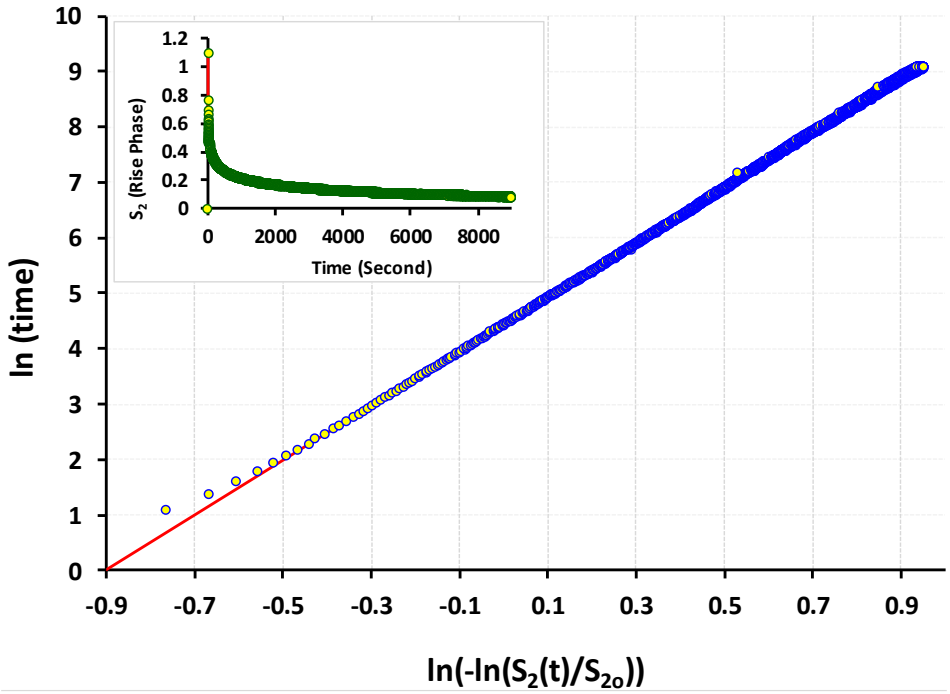

Fig. 4. A logarithmic illustration fit of anisotropy rise according to the stretched exponential function for a 1.5 μm PMMA/DSR13 thin film. The inset (red line) depicts the exponential curve of the stretched exponential function (colour online)

Likewise, the POA dynamic behaviour of decay when the pump beam was switched off is fitted by KWW equation [33],

$$S_2(t) = S_{2o}\left\{1-\exp\left[-\left(\frac{t}{\tau}\right)^{\beta}\right]\right\} \tag{7}$$

where, τ and β are the characteristic decay (relaxation) time and distribution breadth, respectively. Equation 7 was used similarly to Eq. 6 to calculate the relaxation time constant of the samples [34]. This approach was applied to the experimental data of a representative PMMA/DSR13 thin film with 1.5 μm of thickness (Fig. 5), and the results are summarized in Table 1.

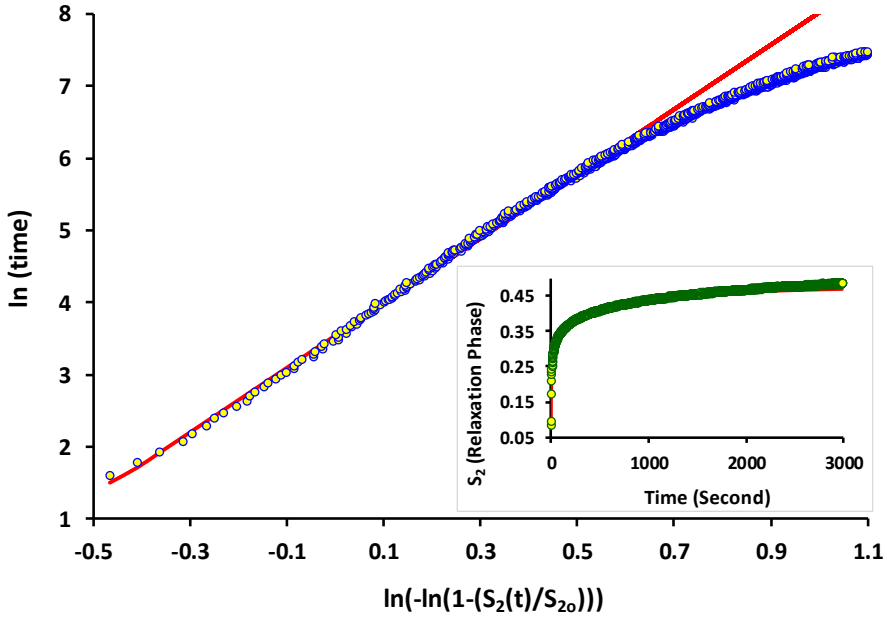

Fig. 5. A logarithmic fit of anisotropy decay to the exponential function for a 1.5 μm PMMA/DSR13 sample. The inset (red line) shows the exponential curve of the exponential function (colour online)

Table 1. Breadth, rise and decay time parameters of PMMA/DSR13 thin films

S_2 Growth Parameters		S_2 Decay Parameters	
β	0.203	β	0.297
τ	86.19	τ	54.45

S_0 is the average optical density, which is dependent on *trans* and *cis* populations. This quantity is calculated from [24],

$$S_{0,\lambda} = OD_m = \frac{1}{3}\left(OD_{//} + 2OD_{\perp}\right) \tag{8}$$

Fig. 6 depicts the dynamic progress of the sample's optical density. It is shown that the optical density rises in a fast fashion during the first 1000 seconds of irradiation. This growth became slower until a photostationary state was reached. Upon switching-off the pump, a relaxation phase in the optical density took place immediately.

However, the optical density did not deteriorate fast, which may take a long time for an isotropic state to be reached. This behaviour of the optical density of the PMMA/DSR13 samples is additional evidence of the photoisomerization processes' dynamic evolution.

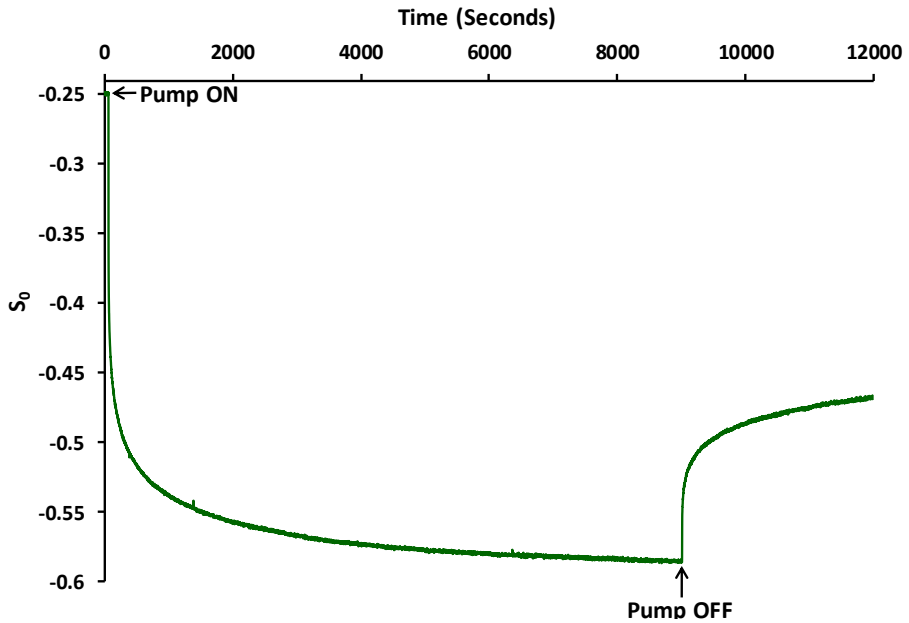

Fig. 6. S_0 dynamic behaviour of PMMA/DSR13 thin film (the pump intensity was 5 mW) (colour online)

Fig. 7 showed that the relative POA (S_2/S_0) is proportional to the order parameter of DSR13 chromophores. (S_2/S_0) increased in a fast manner in the first seconds of irradiation, then slowed afterword until a stationary state was reached. It is also shown that the later isotropic thermal relaxation, at room temperature, of the photoisomers was insignificant, in comparison with the reverse process of the anisotropic photoisomerization that took place instantly after cutting-off the irradiation.

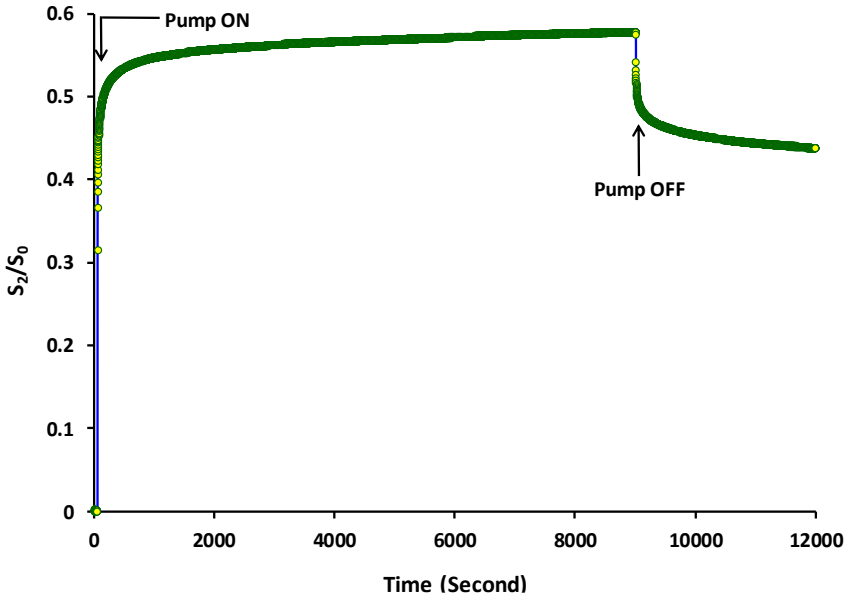

Fig. 7. The relative anisotropy (S_2/S_0) of PMMA/DSR13 samples at a pump intensity of 5 mW (colour online)

Barrett *et al.* [35] studied the *cis* → *trans* thermal isomerisation rates of a few azobenzene dyes (including DSR13 dye) covalently attached as side chains to PMMA network at 10 wt % of dye concentration. They estimated that the thermal relaxation rate of *cis* → *trans* at 1/e is 3.37s for PMMA/DSR13 samples, which is quite smaller than the equivalent value of 88s in our samples. This contrast might be attributed to the difference in the nature of the dye/PMMA bonds, where our system is a guest-host system with no chemical bonding between the dye molecules and the polymer chain, whereas in Barrett *et al.* systems dye molecules were chemically attached to the polymer chain. Also, in our guest-host system the thermal relaxation took place in a very fast fashion once the irradiation was cut-off, so that most of the *cis* molecules relax to the *trans* form, and the slower relaxation mode indicates the local surrounding effect on relaxation for each dye molecule. on the other hand, their results showed that the

fast decay was more than 99.5% complete after 3 s, which is different in our system. Moreover, the rate of *cis* → *trans* thermal back decay is usually temperature dependent (as well as its dependence on the free volume available for isomerisation to occur). Therefore, the chemical and geometrical structure plays a critical role in the thermal relaxation process. For example, the closest chemical and geometrical structure for DSR13 is DSR1. They are only different from each other by the Cl cation that exists in DSR13. This difference manifests in different values of their dipole moment and in their thermal *cis* → *trans* relaxation parameters. The dipole moment of DSR1 and DSR13 are 9.1 and 9.3 Debye, respectively [36]. This difference may explain the faster relaxation fashion in PMMA/DSR13 sample in comparison with PMMA/DSR1 samples which were studied by Blanchard [37], who found that for a guest-host system of PMMA/DSR1 the thermal relaxation parameters were β=0.23±0.01 and τ=1100±200s. This can be explained in the light of *trans* → *cis* → *trans* isomerisation cycle, where upon pumping the *trans* molecules into the *cis* state, they have two ways of relaxing back to the original *tans* state. First, they can relax back to the same original *trans* state and original spatial position so that they are, again, enrolled in the *trans* → *cis* → *trans* process. Or second, the *cis* molecules relax back to *trans* state but in a new spatial position so that they are in a different plane from the original one according to the angular redistribution model and therefore they are less likely to undergo the *trans* → *cis* → *trans* process. The new position for these trans molecules can be small enough to prevent them redistribute thermally in a short time so that this reorientational process takes a long time to have the guest-host system in a thermodynamically stable state.

4. Conclusion

POA of PMMA/DSR13 samples occurs as a result of the competition between AHB by polarized light, and AR during the photoisomerization, the photoisomer's lifetime, and the photoinduced (or spontaneous) return to the stable isomeric form.

In the first seconds, the AHB was predominant, and the AR emerged slowly in the following minutes. The POA anisotropy in PMMA/DSR13 samples did not vanish instantaneously at the moment of switching off the pumping beam. Furthermore, the dynamic behaviour of the POA growth when switching on the pumping beam and deterioration after cutting it off could be fitted by KWW exponential equations, which indicated a complex increase and relaxation behaviour. The changes could be attributed to the contribution of the local environment around each dye molecule inside the polymeric assembly.

The presented results proved the usefulness of the PMMA/DSR13 hybrid structure as thin films in photonics and optoelectronic applications.

Acknowledgments

The authors would like to acknowledge the Director General of the AECS, for his great support throughout this research. The authors would like, also, to thank the Head of the Department of Physics, Mr. A. Salloum, and Mr. H. Othman for his help and advice.

References

[1] Z. Sekkat, P. Prêtre, A. Knoesen, W. Volksen, V. Y. Lee, R. D. Miller, J. Wood, W. Knoll, J. Opt. Soc. Am. B **15**, 401 (1998).
[2] I. G. Marino, R. Raschell, P. P. Lottici, D. Bersani, C. Razzetti, A. Lorenzi, A. Montenero, J. Sol-Gel Sci. Technol. **37**, 201 (2006).
[3] D. H. Choi, Y. K. Cha, Bull. Korean Chem. Soc. **23**(3), 469 (2002).
[4] A. Natansohn, S. Xie, P. Rochon, Macromolecules **25**, 5531 (1992).
[5] T. Shim, S. Kim, D. Kim, M. Oh-e, Journal of Applied Physics **110**, 063532 (2011).
[6] H. Ono, F. Takahashi, A. Emoto, Journal of Applied Physics **97**, 053508 (2005).
[7] A. Namdar, H. Tajalli, Laser Physics **14**(12), 1520 (2004).
[8] D.-K. Yang, S.-T. Wu, Fundamentals of Liquid Crystal Devices, Wiley, Chichester, 378 (2006).
[9] V. G. Chigrinov, V. M. Kozenkov, H.-S. Kwok, Photoalignment of Liquid Crystalline Materials: Physics and Applications, John Wiley & Sons Ltd, The Atrium, Southern Gate, Chichester, 219 (2008).
[10] K. Paeng, H.-N. Lee, S. F. Swallen, M. D. Ediger, J. Chem. Phys **134,** 024901 (2011).
[11] S. V. Pasechnik, A. V. Dubtsov, D. V. Shmeliova, D. A. Semerenko, V. G. Chigrinov, M. A. Sinenko, Alexei D. Kiselev, Phys. Rev. E **82**(1), 011702 (2010).
[12] M. Russo, S. E. J. Rigby, W. Caseri, N. Stingelin, Adv. Mater. **24**, 3015 (2012).
[13] C. Weder, C. Sarwa, A. Montali, C. Bastiaansen, P. Smith, Science **279**, 835 (1998).
[14] A. Montali, C. Bastiaansen, P. Smith, C. Weder, Nature **392**, 261(1998).
[15] P. P. Markowicz, M. Samoc, J. Cerne, P. N. Prasad, A. Pucci, G. Ruggeri, Optics Express **12**, 5209 (2004).
[16] A. Piqué, R. C. Y. Auyeung, J. L. Stepnowski, D. W. Weir, C. B. Arnold, R. A. McGill, D. B. Chrisey, Surf. Coat. Tech. **163 –164**, 293 (2003).
[17] V. P. Toshchevikov, M. Saphiannikova, G. Heinrich, J. Chem. Phys. **137**, 024903 (2012).
[18] S. Bauer, J. Appl. Phys. **80**(10), 5531 (1996).
[19] A. Pucci, M. Bertoldo, S. Bronco, Macromol. Rapid Commun. **26**, 1043 (2005).
[20] M. Pokrzywnicka, D. J. Cocovi-Solberg, M. Miró, V. Cerdà, R. Koncki, Ł. Tymecki, Anal. Bioanal. Chem. **399**, 1381 (2011).

[21] A. Charas, J. Morgado, Curr. Phys. Chem. **2**, 241 (2012).
[22] R. H. El Halabieh, O. Mermut, C. J. Barrett, Pure Appl. Chem. **76**(7–8), 1445 (2004).
[23] C. Cojocariu, P. Rochon, Pure Appl. Chem. **76**(7–8), 1479 (2004).
[24] M. Fischer, A. El-Osman, P.-A. Blanche, M. Dumont, Synth. Met. **115**, 139 (2000).
[25] Y. Wu, M. Xing, Y. Ding, Z. Lin, M. Zhang, Chemical Physics Letters **743**, 137163 (2020).
[26] A. Petris, P. Gheorghe, I. Rau, A.-M. Manea-Saghin, F. Kajzar, European Polymer Journal **110**, 130 (2019).
[27] A. Szukalski, K. A. Haupa, A. Adamow, Y. Cheret, R. Hue, A. El-Ghayoury, B. Sahraoui, D. Pisignano, J. Mysliwiec, A. Camposeo, J. Phys. Chem. C **124**, 25465 (2020).
[28] G. A. Alharshan, H. A. Saudi, S. A. M. Issa, H. M. H. Zakaly, H. M. Gomaa, Optics & Laser Technology **181**, 111690 (2025).
[29] B. Abbas, M. Alshikh Khalil, Acta Phys. Pol. A **115**(5), 857 (2009).
[30] C. R. Mendonca, L. Misoguti, A. A. Andrade, S. B. Yamaki, V. D. Dias, T. D. Z. Atvars, O. N. Oliveira Jr., Opt. Mater. **30**, 216 (2007).
[31] Y. Wang, C. H. Wang, J. Appl. Phys. **98**, 103526 (2005).
[32] S. Liu, W. L. Wang, C. C. Fang, T.-H. Huang, C. C. Hsu, J. Appl. Phys. **97**, 013103 (2005).
[33] G. Williams, D. C. Watts, Trans. Faraday Soc. **66**, 80 (1970).
[34] K. D. Singer, L. A. King, J. Appl. Phys. **70** (6), 3251 (1991).
[35] C. Barrett, A. Natansohn, P. Rochon, Chem. Mater. **7**, 899 (1995).
[36] S. Mukamel, Principles of Nonlinear Optical Spectroscopy, Oxford University Press, New York, 454 (1995).
[37] P. M. Blanchard, Ph.D. Thesis, The University of Reading (1993).

*Corresponding author: pscientific34@aec.org.sy